Memorandum

To:	E. Bryerton	K. Crady
	G. Ediss	N. Horner
	A. R. Kerr	D. Koller
	G. Lauria	S.-K. Pan
	K. Saini	D. Thacker
cc:	J. Webber	
From:	J. Effland	
	R. Groves	
Date:	2003-04-16	

Revisions:			
	2002-11-26	jee	Initial Draft
	2003-02-27	jee	Draft updated with data from mixer-preamp UVA10-01-L-1343C-1202-2-HI-C14-L59-3-375C-104-M375P.05
	2003-04-16	jee	Measurement technique changed to use chopper wheel and square law detector for mixer UVaV-L568A-2-F6-2-B3-371C-01 + IF4-12P.04

Subject: Saturation Measurements of Single-Ended SIS Mixer-Preamp for ALMA Band 6

1 Introduction

Saturation of ALMA receivers must be carefully characterized to achieve the array's stringent overall absolute flux accuracy goal of 1%[1]. Saturation levels between 0.5% and 1.9% were measured using three different ALMA Band 6 single-ended SIS mixers with integrated preamp[2]. Some of the data agrees with theoretical values calculated by A.R. Kerr[3]. This memo documents equipment setups, procedures, and the results from a series of mixer saturation measurements.

Two different measurement techniques were used to measure saturation and are described here. Initially, the HP 436 power meter averaged the noise powers for a number of seconds at each state of the chopper wheel. To reduce the variance in the data, a second technique was employed by measuring noise power with the square law detector with the chopper wheel spinning at 12 revolutions per second.

2 History

A.R. Kerr's ALMA Memo 401 includes procedures for determining the saturation from noise of SIS mixers by measuring the change in level of an injected signal while hot and cold loads are alternately placed in the path of the receiver's input beam. That procedure was used at the NRAO's CDL to measure the saturation of an ALMA Band 6 single-ended SIS mixer with integrated preamp as documented in this memo.

3 Slow Power Meter Measurements

The equipment configuration for measuring the saturation of mixer-preamp UVaV-L568A-2-F6-2-B3-371C-01 + IF4-12P.04 with the power meter is shown in Figure 1. Another mixer-preamp, UVA10-01-L-1343C-1202-2-HI-

C14-L59-3-375C-104-M375P.05 was measured using the almost identical setup shown in Figure 2 except that the YIG filter was not present in the prototype ALMA LO system. The prototype ALMA LO system[4] provided the local oscillator for the mixer and the injected signal was generated from a Gunn oscillator that was stabilized in frequency using a XL 800A Gunn Lock system. It was hoped that locking the Gunn oscillator would reduce amplitude variations in the injected signal that arise from frequency changes. Subsequent testing with free-running Gunns showed no advantage to using the Gunn Lock system, except to keep the injected signal from drifting out of the passband of the 240 MHz wide IF filter.

Total power was band limited with a 10.24 GHz band pass filter exhibiting a 3-dB bandwidth of 240 MHz and measured with an Agilent EPM 441 power meter and an HP 8484A power head. The signal and LO frequencies were adjusted so that the signal fell inside the passband of the 10.24 GHz bandpass filter. The control software calculated a running average of power measurements and the mean was stored in spreadsheet cells after the standard error decreased to less than 10^{-8}.

Saturation is calculated from the ratio of two power measurements: First, signal-plus-noise power is measured when the receiver's beam is directed to a hot load, and then signal-plus-noise power is measured again when the receiver's beam is directed to a cold load. Noise powers when no signal is present are also measured for each case and subtracted from the respective signal-plus-noise powers.

$$Sat_{\%} = 100 \times \left(\frac{P_{sig,hot} - P_{hot}}{P_{sig,cold} - P_{cold}} \right) - Sat_{PostMxr}$$

where

$Sat_{\%}$	is the saturation level in percent,
$P_{sig,hot}$	is the signal power measured at the filter output when a hot load is inserted in the path of the receiver beam,
$P_{sig,cold}$	is the signal power measured at the filter output when a cold load is inserted in the path of the receiver beam,
P_{hot}	is the noise power measured at the filter output with the signal off when a hot load is inserted in the path of the receiver beam,
P_{cold}	is the noise power measured at the filter output with the signal off when a cold load is inserted in the path of the receiver beam,
$Sat_{PostMxr}$	is the saturation level for the amplifiers that following the mixer-preamp.

To measure the saturation of the two IF amplifiers located downstream from the mixer-preamp, the test signal was injected after the mixer-preamp into Port 4 shown in the block diagrams. The 6-way IF switch allowed the signal from Port 4 and the noise from the mixer-preamp to be injected simultaneously into the latter IF stages. Impedance mismatch effects from these two 50 ohm lines in shunt were ignored. The saturation of the post-mixer-preamp stages, measured over a period of time, averaged 0.25% as shown in Figure 4.

To determine the stability of the measurement, total noise power was recorded and the saturation was calculated and plotted as a function of time. Figure 5 shows saturation measurements, with no correction for the signal off case, for a particular LO frequency and injected signal frequency. In Figure 5, the sinusoidal variation was of interest, and during investigation of that phenomenon, no corrections were made for post mixer-preamp saturation levels or for noise powers when the signal was turned off.

3.1 Measurement of mixer-preamp UVaV-L568A-2-F6-2-B3-371C-01+IF4-12P.04

Figure 5 shows that the saturation varies sinusoidally at a nearly-constant 5.5-minute period and that the phase of the sinusoid changes when the cold load is filled. Several weeks were spent attempting to determine the source of the sinusoidal changes and included investigating the following:

a) changes in either hot- or cold-load physical temperatures,
b) time-varying changes in the saturation of amplifiers following the mixer-preamp,
c) changes in LO or injected signal power levels, and
d) interfering signals leaking into the system.

LO power levels were monitored by using a HP W8486A power head to measure and record the level of the 100-GHz signal on the automated LO plate. An independent check of LO level was made by monitoring SIS mixer current. Finally, the temperature of the hot load was also recorded. All three of these parameters are plotted on the accompanying figures measured with the power meter.

The angle of the mirror that reflects the receiver beam into the cold load was changed and more data were recorded and plotted in Figure 6. Changing the mirror angle moves the region of the cold load illuminated by the beam and also changes the electrical length from the cold load to the receiver. The significant difference between the saturation measured in Figure 5 and that of Figure 6 is that the period of the sinusoid now changed each time the cold load was filled. Based on these observed changes, it was concluded that the periodicity in saturation results from an interaction between the mixer and the liquid nitrogen cold load. To eliminate this effect, all saturation data was calculated from the long-term mean of the measured sinusoidally-varying data.

A basic premise of this measurement technique is that the injected signal power is sufficiently low that it doesn't affect the saturation point of the receiver. To confirm this, the level of the injected signal was increased by 10 dB and, as shown in Figure 7, no changes to the measured saturation were observed.

Figure 8 is a saturation measurement at an LO frequency of 280 GHz and shows essentially the same saturation level as the 253 GHz data.

Figure 9 summarizes the results for mixer-preamp UVaV-L568A-2-F6-2-B3-371C-01 + IF4-12P.04 for several LO frequencies.

3.2 Measurement of mixer-preamp UVA10-01-L-1343C-1202-2-HI-C14-L59-3-375C-104-M375P.05

Figure 10 shows saturation results measured using mixer-preamp UVA10-01-L-1343C-1202-2-HI-C14-L59-3-375C-104-M375P.05. The saturation averages about 1.9% (excluding the saturation contribution from the latter stages) compared to about 0.75% for mixer-preamp UVaV-L568A-2-F6-2-B3-371C-01+IF4-12P.04. Figure 11 shows the saturation of the amplifier stages following the mixer-preamp. This was measured two ways: First, the setup was kept identical to the configuration used to measure the mixer-preamp saturation as presented in Figure 11. To determine if the final amplifier was contributing to this latter-stage saturation, a 7-dB attenuator was inserted at the input to this amplifier and the pin-diode attenuator was adjusted to maintain the same nominal -22 dBm power level at the power head. Within the measurement error, both measurements show essentially the same results, although it appears that saturation of the IF system is slightly less when the signal to the final amplif8er stage is reduced.

4 Measurement with a Rapidly Rotating Chopper Wheel

The previous saturation data in this report were collected using the chopper wheel and a power meter that typically averaged 10 measurements for each hot and cold load position of the chopper to reduce the standard error below a preset threshold. This meant that the chopper dwelled for many seconds at each hot and cold load position, so stability of the overall system gain was paramount to reducing variance in the saturation data. Gain stability is difficult to achieve when the overall gain is ~85 dB, so A.R. Kerr suggested increasing the speed of the chopper wheel and using the square law detector to measure total power changes.

The equipment setup, Figure 3, shows that the power meter is replaced by a square law detector consisting of a NRAO design by A. R. Kerr with an updated tunnel diode detector that covers the 4-12 GHz band[5]. The shopper was spinning at 12 revolutions per second and the two hot and cold load positions per revolution yields 24 measurements per second. The square law detector averages 2 sets of 256 samples collected during each hot and cold load state[6]. Future work is planned to replace the square law detector with a modern Agilent power meter reading at 40, 200, or 400 measurements per second.

4.1 Results

Figure 12 and Figure 13 show saturation results using the rapidly-rotating chopper and square law detector with the LO frequency of 230 GHz and the signal injected into the lower sideband. Variance is significantly reduced using this approach compared with the slower power meter data presented earlier in this report. The ripple in the data is thought to be from an interaction between the surface of the cold load's liquid nitrogen and the mixer as the LN2 boils off. The phase of the ripple changes when the cold load is refilled, and the period of the ripple changes when the angle of the mirror above the cold load changes.

At the beginning and end of most measurements, saturation of the IF system was measured by injecting a signal into the coupler mounted at the input of the cold IF amplifier as shown in Figure 3. Most measurements show the saturation of the latter IF stages are at about the 0.5% level, but several (Figure 16, Figure 21, and Figure 22), show the IF stages saturating at the 0.7% level. The cause of these discrepancies is unknown.

We confirmed that the injected signal did not contribute significantly to mixer-preamp saturation by reducing the injected signal by 4 dB and noting that the saturation level remained constant. This was measured near the end of the data acquisition (~ 18:50 hours) in Figure 22.

The saturation measurements shown in Figure 17 and Figure 18 at a LO frequency 253 GHz show considerable drift. Figure 23 and Figure 24 are previous saturation measurements with the raw square law detector voltages superimposed on the graphs. The raw square law detector voltages exclude the no-signal offset voltages. The ripple, whose cause is unknown, in the detected voltage shown in Figure 23, has about a 2-minute period. The largest drift in saturation is shown in Figure 23 and it is apparent that the difference between the signal voltages for the hot and cold load cases decrease with time. Figure 24 shows detected voltages for a sweep that exhibits little saturation drift, and the magnitude of the ripples in the detected voltage is less. Further investigation of the drift phenomenon is planned for future saturation measurements.

The voltage corresponding to no signal is nearly inconsequential, because it is at most 20 mV, or a factor of 100 less than the voltages detected with the signal, so it's measured just once at the beginning of the measurement using a hot and cold load at the receiver input.

4.2 Mixer-Preamp Gain vs. LO Power

To determine if the chopper wheel was causing a varying impedance mismatch at the mixer-preamp, the mixer current was monitored as the chopper wheel was slowly rotated from hot to cold load. We concluded that the

chopper wasn't significantly modulating mixer-preamp gain because the mixer current was constant for both states of the chopper.

The gain of the mixer-preamp was also measured as a function of mixer current by recording total noise powers when the chopper was in the hot and cold load positions for different LO powers, which are directly related to mixer currents. The relative gain, ΔG, is found from the ratio of two noise power differences, and since each noise power is a function of gain, G_{Ijx}, Boltzmann's constant, k, system noise temperature, T, and IF bandwidth, B

$$\begin{aligned}\Delta G &= \frac{P_{hot,Ij_1} - P_{cold,Ij_1}}{P_{hotIj_{ref}} - P_{coldIj_{ref}}} \\ &= \frac{G_{Ij_1}\left(kT_{hot}B - kT_{cold}B\right)}{G_{Ijref}\left(kT_{hot}B - kT_{cold}B\right)} \\ &= \frac{G_{Ij_1}}{G_{Ijref}}\end{aligned}$$

where each of the P's represents total noise power from the receiver connected to:

$P_{hot,Ij1}$ = hot load with mixer current 1
$P_{cold,Ij1}$ = cold load with mixer current 1
$P_{hot,Ijref}$ = hot load with reference mixer current
$P_{cold,Ijref}$ = cold load with reference mixer current.

A reference mixer current of 50 μA was used for the results, shown in Figure 25.

5 Acknowledgments

The authors wish to acknowledge and thank our colleagues A.R. Kerr, John Webber, S.-K. Pan, N. Horner, and W. K. Crady for their assistance in these measurements.

[1] Holdaway, Wootten, Payne, Vaccari *et al*., "Calibration", Chapter 3 of ALMA Project Book, Rev 2001-02-06, Available at http://www.alma.nrao.edu/projectbk/construction/

[2] E. F. Lauria, A. R. Kerr, M. W. Pospieszalski, S.-K. Pan, J. E. Effland, and A. W. Lichtenberger, "A 200-300 GHz SIS Mixer-Preamplifier with 8 GHz IF Bandwidth," 2001 IEEE International Microwave Symposium Digest, pp. 1645-1648, 2001-05. Available as ALMA Memo 378 at http://www.alma.nrao.edu/memos/.

[3] A.R. Kerr, "Saturation by Noise and CW Signals in SIS Mixers," ALMA Memo 401, 2001-12-15, Available at http://www.alma.nrao.edu/memos/

[4] E. W. Bryerton, S. K. Pan, D. Thacker, and K. Saini, "Band 6 Receiver Noise Measurements Using a Pre-Prototype YIG-Tunable LO, ALMA Memo 436, 2002-09-02, Available at http://www.alma.nrao.edu/memos/

[5] J. Effland and W. Crady, "Square Law Detector Upgrades," NRAO CDL Memo, 2002-05-02. Available at http://www.cv.nrao.edu/~jeffland/SquareLawDetResults.pdf

[6] J. Effland, "Coax Switch Controller, Refrigerator Controller, and Chopper Wheel Design Document," 2000-09-21, Version 1.72. Available at http://www.cv.nrao.edu/~jeffland/SwitchControlHardwareDesign.pdf.

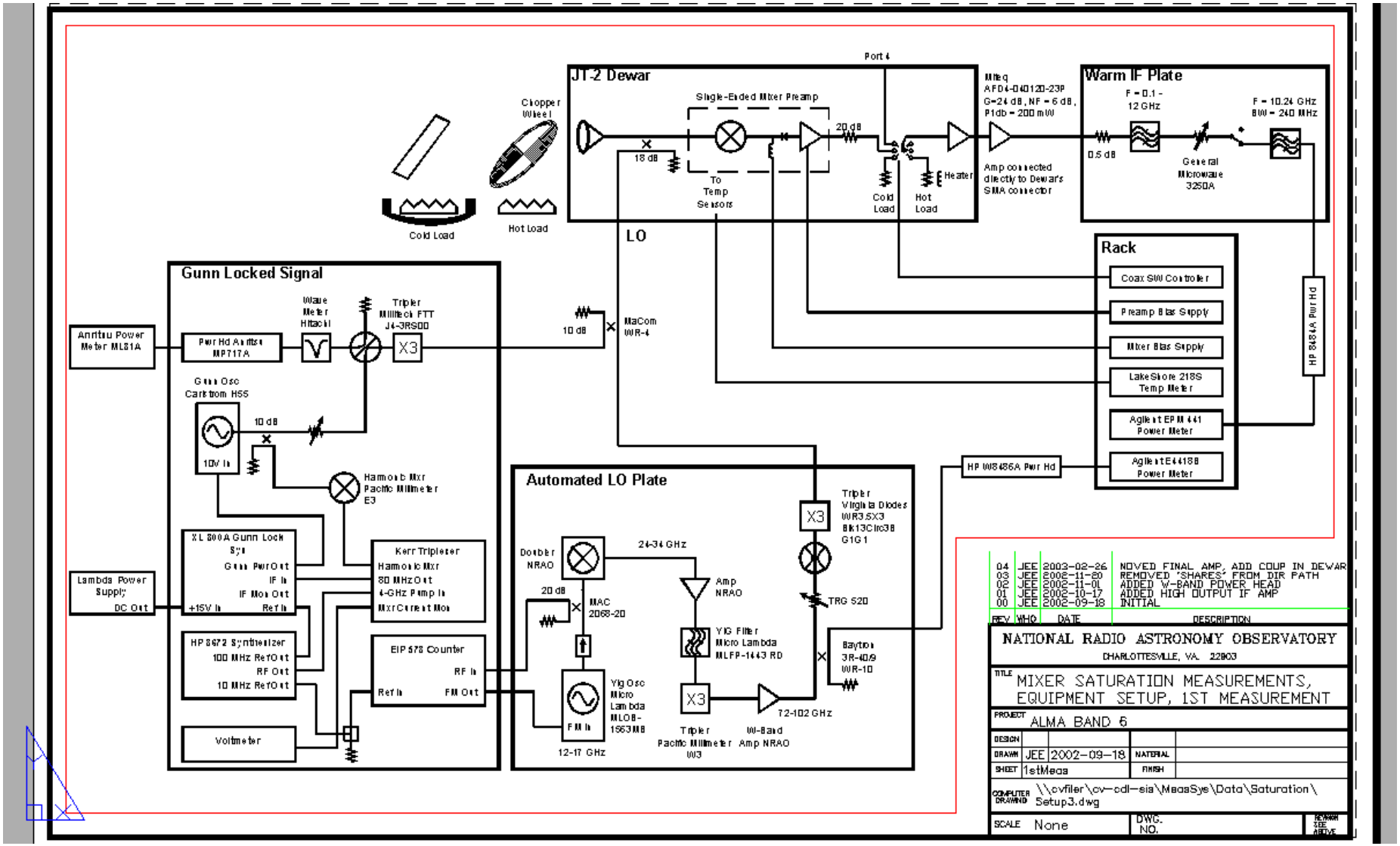

Figure 1: Mixer Saturation Measurement Setup for Mixer-Preamp UVaV-L568A-2-F6-2-B3-371C-01 + IF4-12P.04. This setup uses power meter with chopper wheel paused at hot and cold load positions.

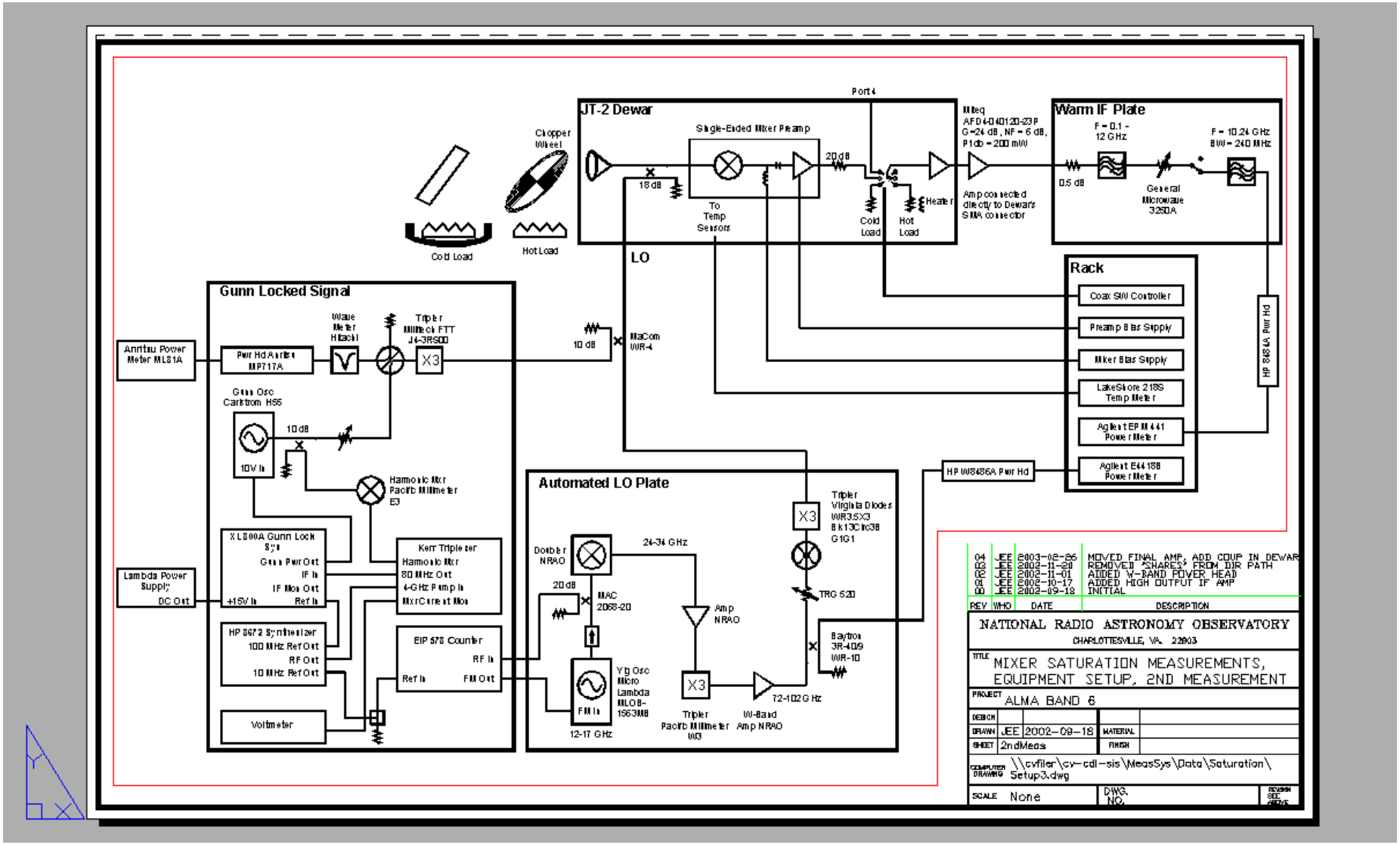

Figure 2: Mixer Saturation Measurement Setup for Mixer-Preamp UVA10-01-L-1343C-1202-2-HI-C14-L59-3-375C-104-M375P.05. This setup uses power meter with chopper wheel paused at hot and cold load positions.

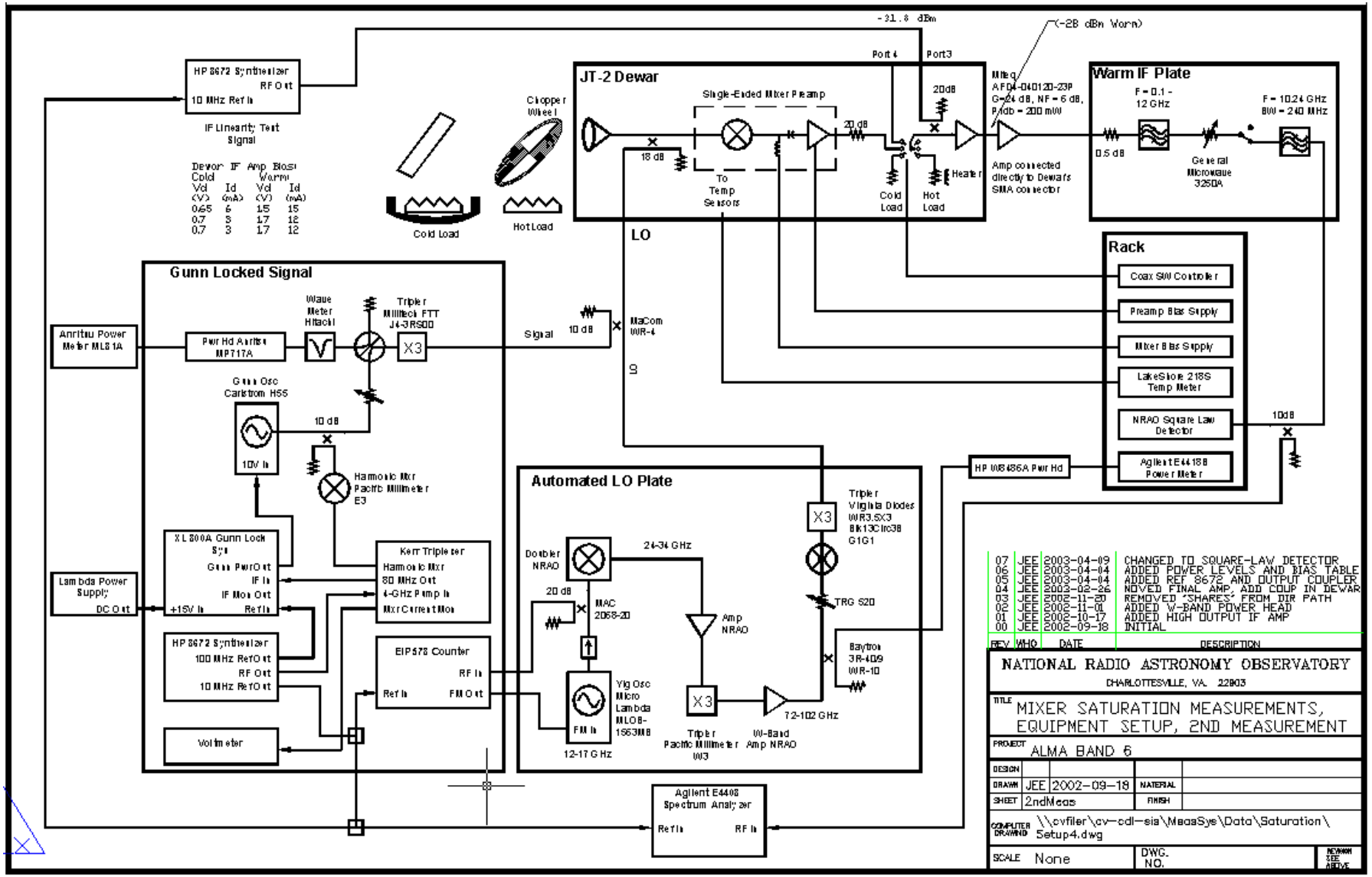

Figure 3: Mixer Saturation Measurement Setup for Mixer-Preamp UVA10-01-L-1343C-1202-2-GH-C14-L62-1-375C-103-M375P.15. This setup uses a square law detector and the chopper wheel rotating at 12 revolutions per second. Phase locking of the injected signal was not always necessary. See text for details

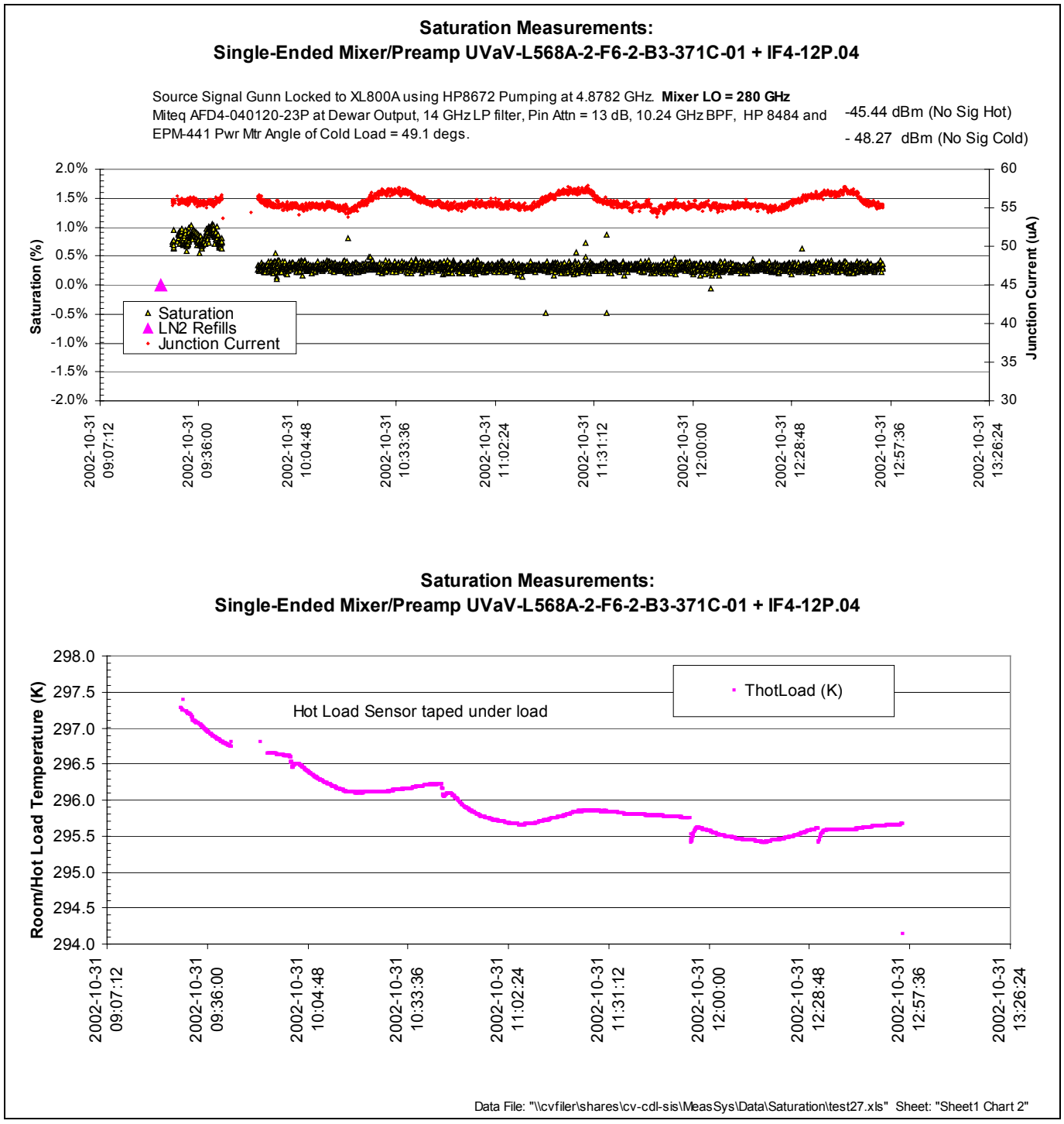

Figure 4: Saturation of latter stages obtained by injecting signal after mixer-preamp into "Port 4" shown Figure 1. This data shows the latter stages contribute about 0.3% to the saturation.

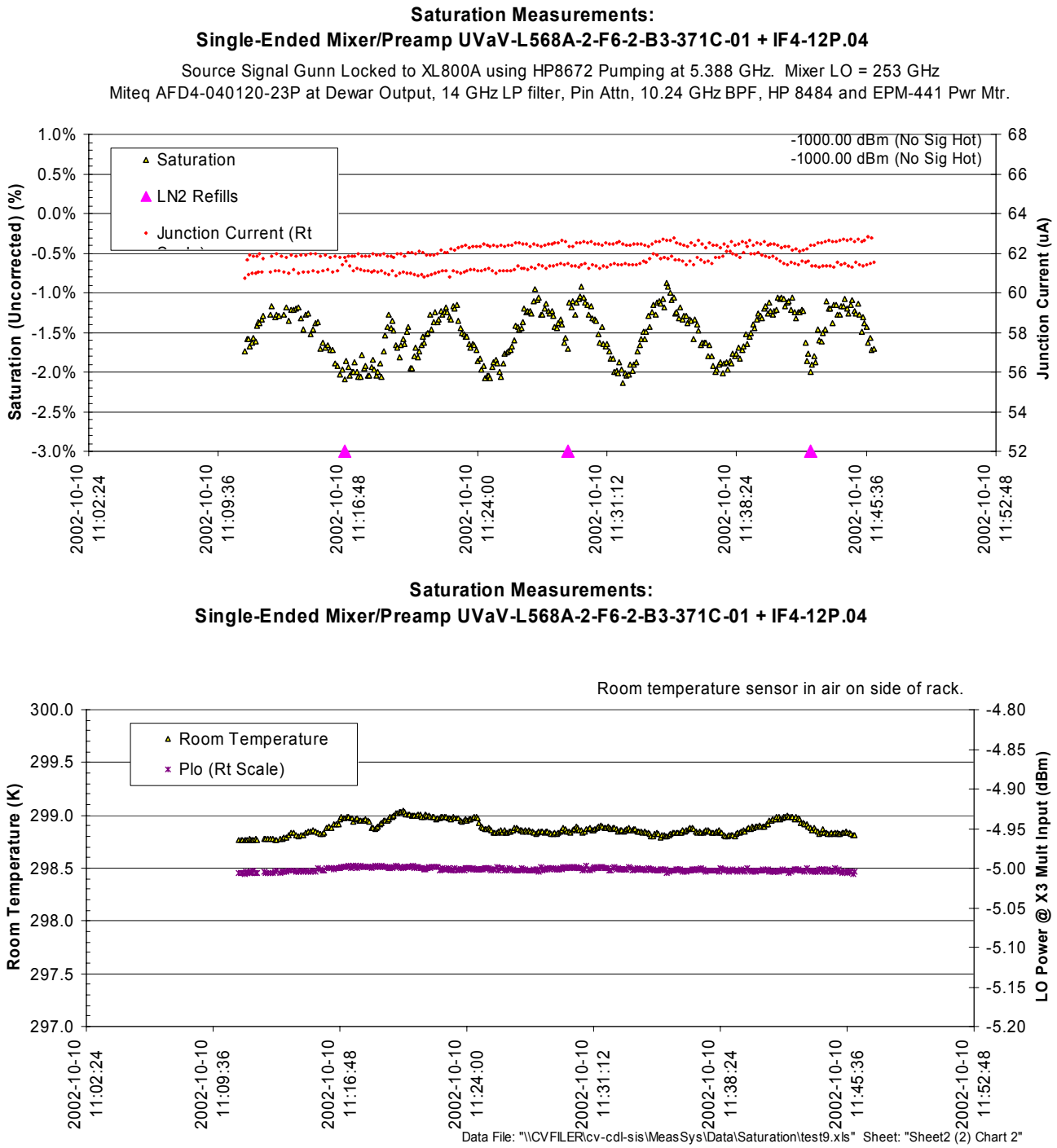

Figure 5: Phase change of ripple in saturation data when cold load is refilled. Cold load mirror angle at 30°.

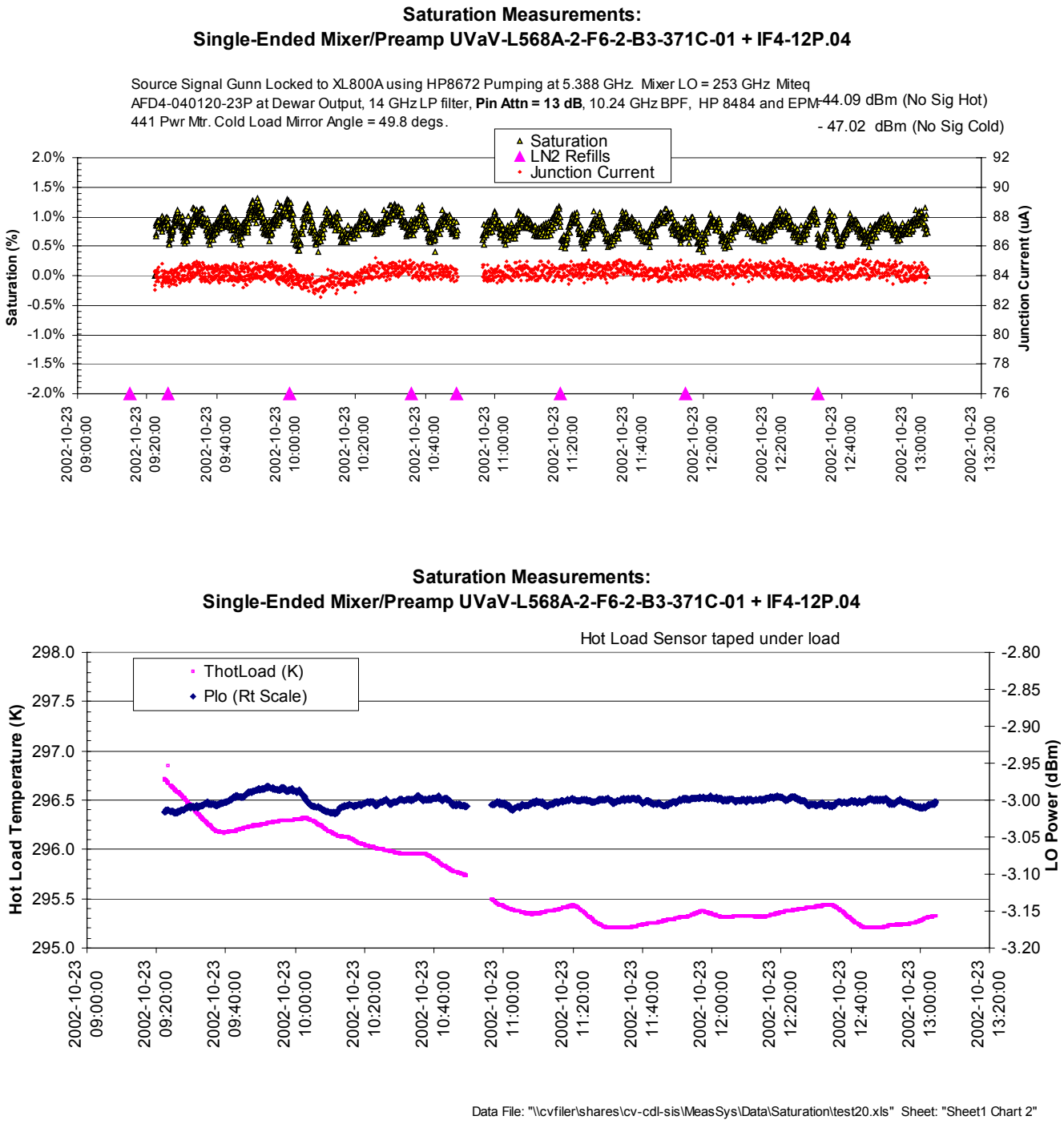

Figure 6: Frequency change of ripple in saturation data when cold load is refilled. Cold load mirror angle at 44°.

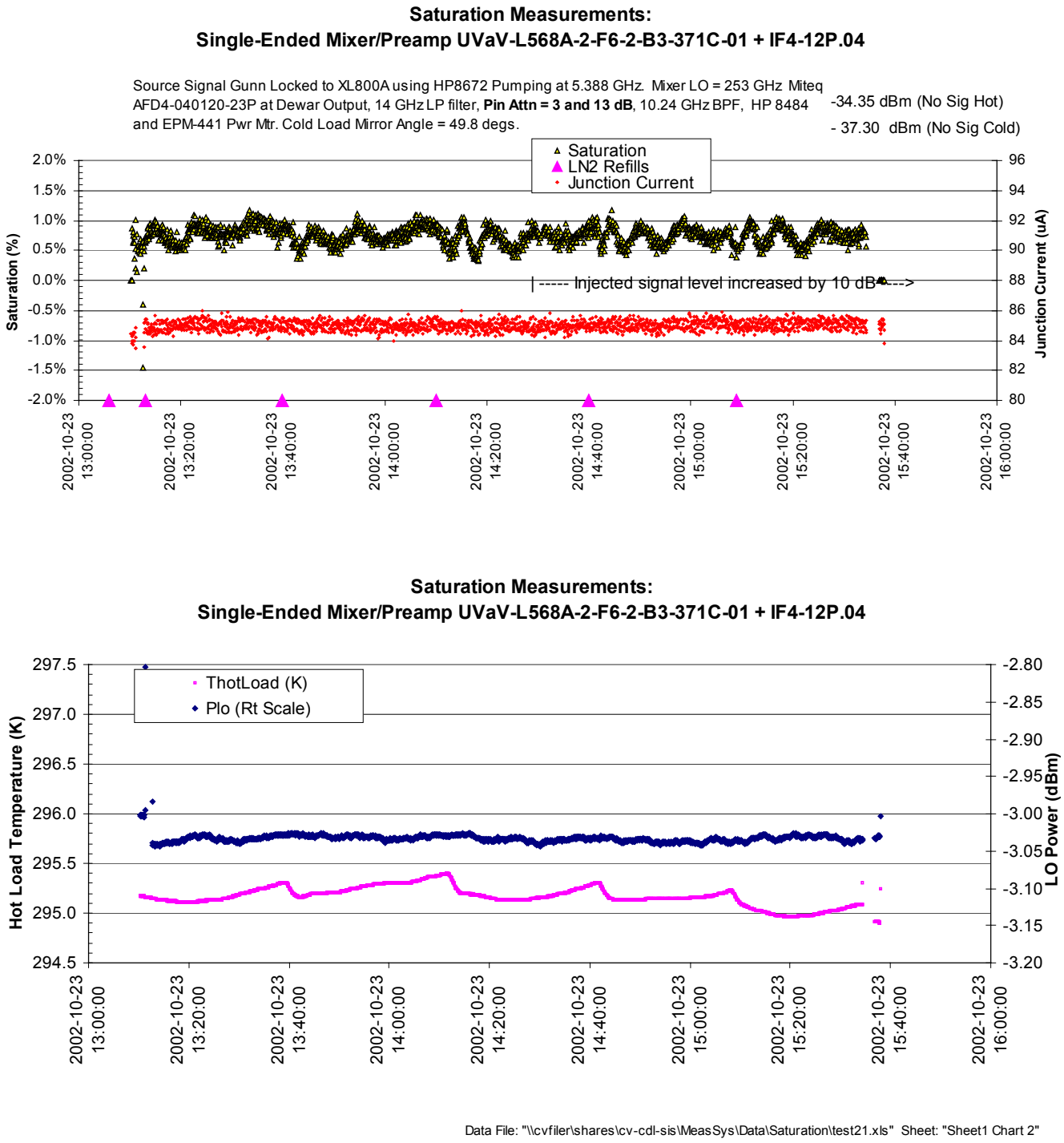

Figure 7: No change in saturation level with 10-dB increase in injected signal

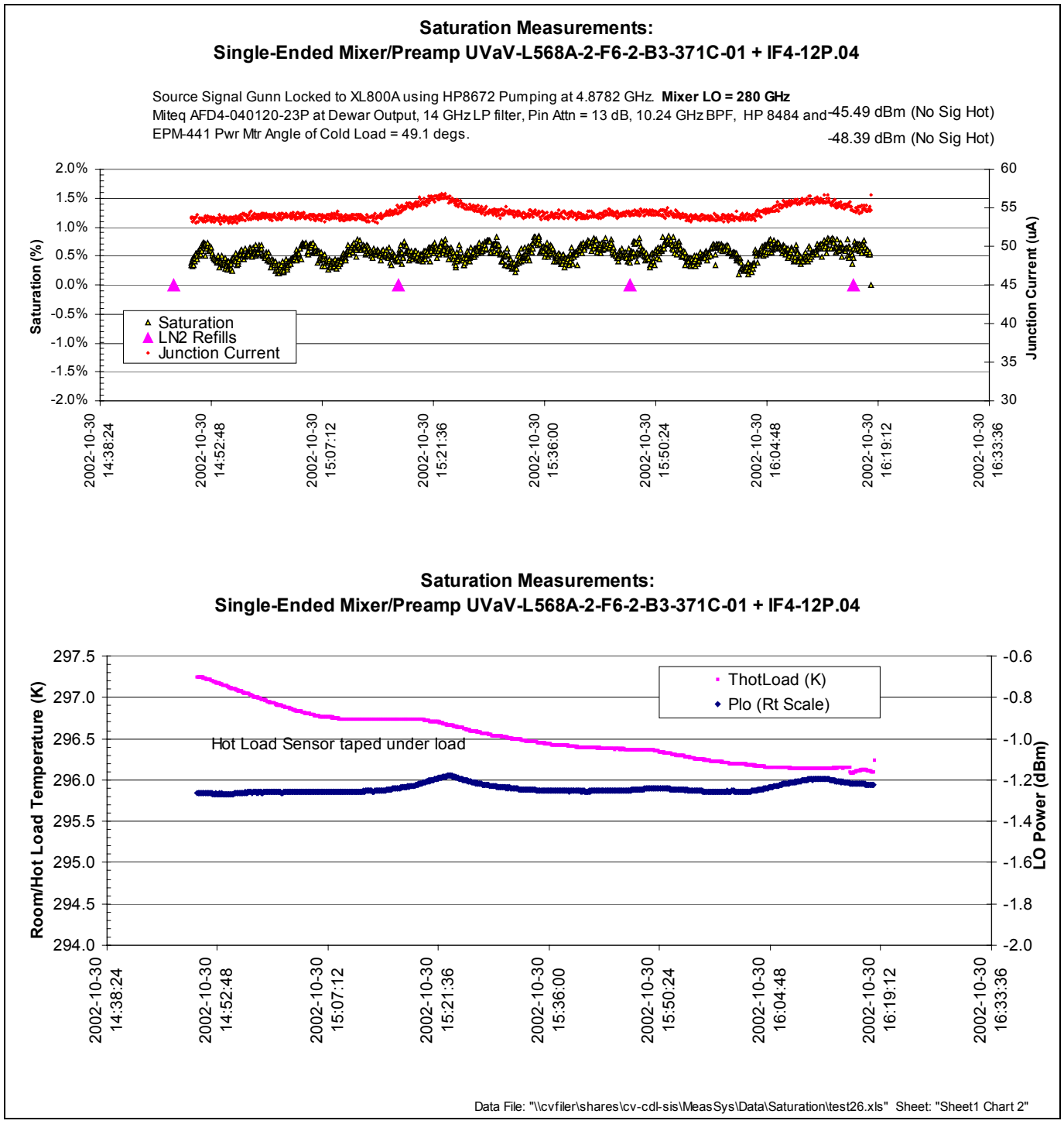

Figure 8: Saturation with LO = 280 GHz

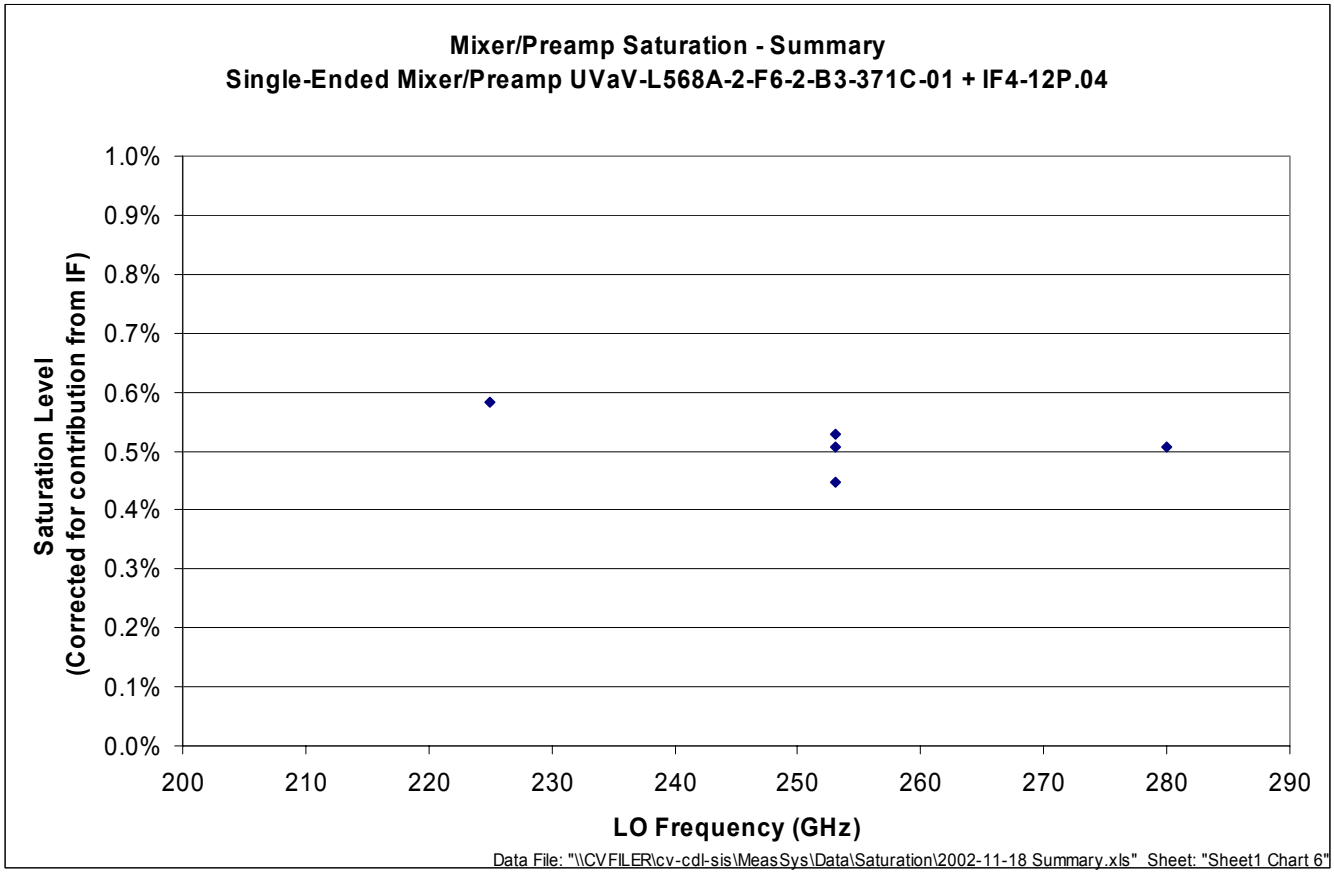

Figure 9: Summary data for single-ended mixer-preamp saturation *vs.* LO frequency. Saturation has been corrected by 0.31% contribution from IF stages.

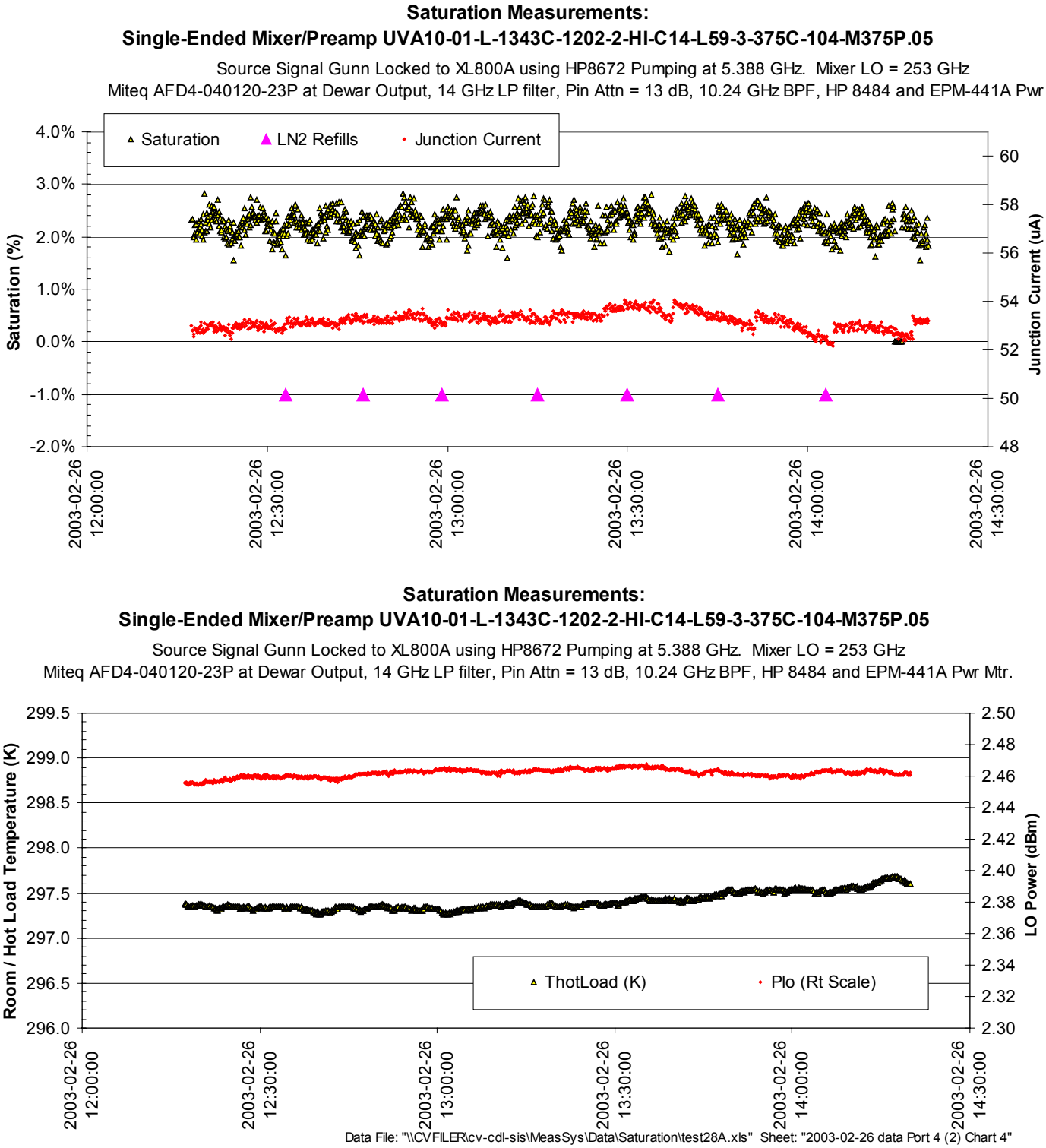

Figure 10: Saturation of UVA10-01-L-1343C-1202-2-HI-C14-L59-3-375C-104-M375P.05 shows that this mixer-preamp has about 1.9% saturation (excluding 0.5% from latter stages)

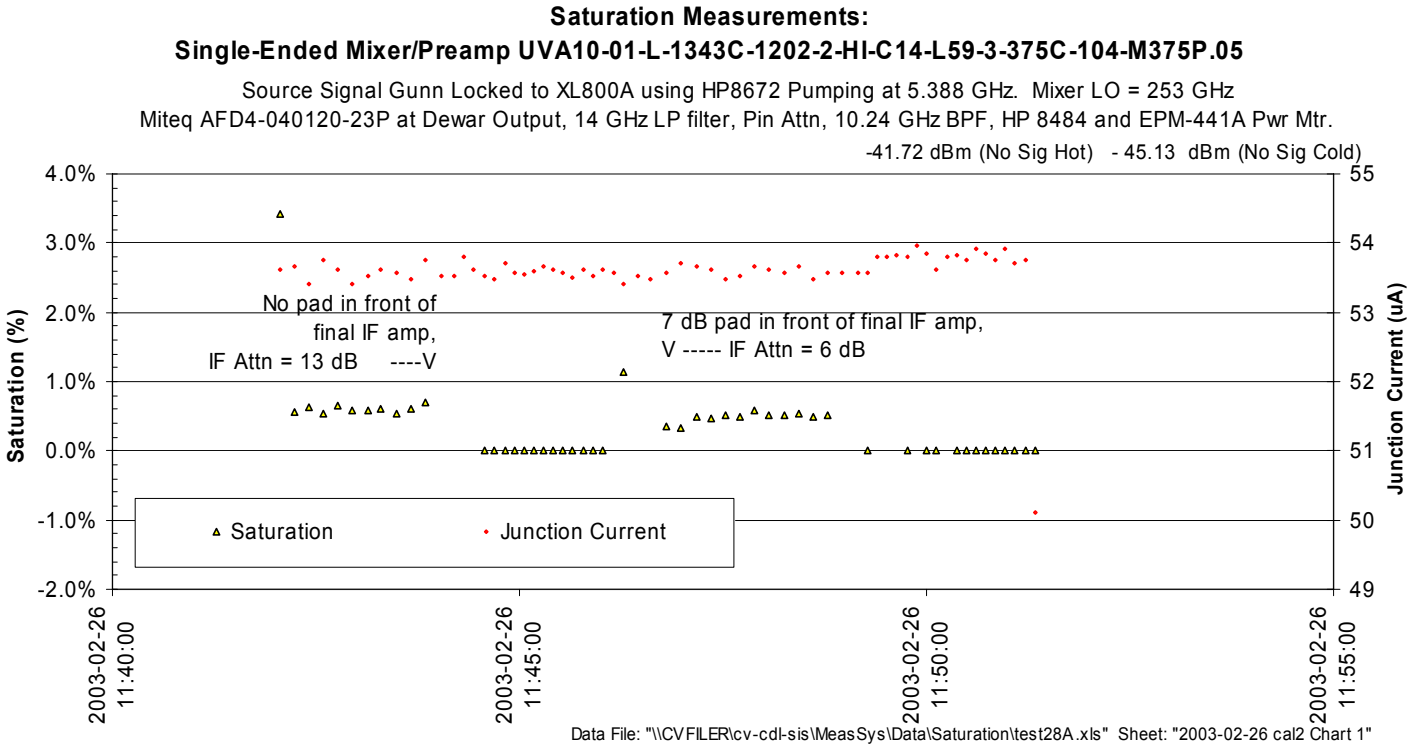

Figure 11: Saturation of latter stages obtained by injecting signal after mixer-preamp into "Port 4" shown Figure 2. The latter stages contribute about 0.5% to the total measurement.

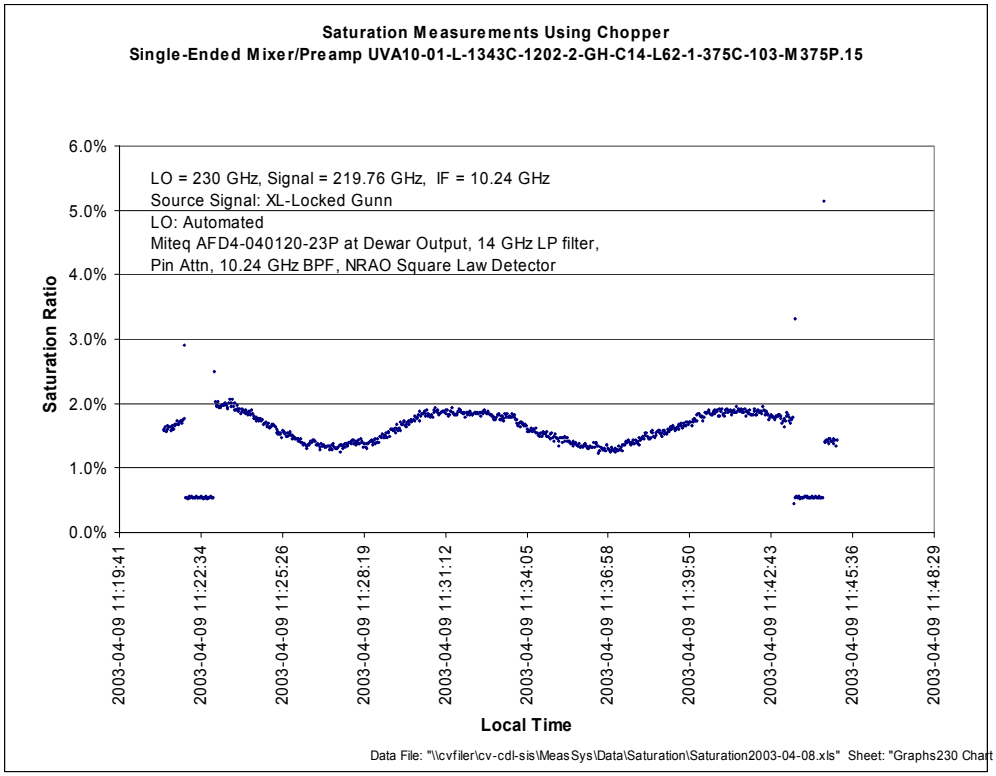

Figure 12: Saturation with LO = 230 GHz, LSB, using square law detector and fast chopper wheel.

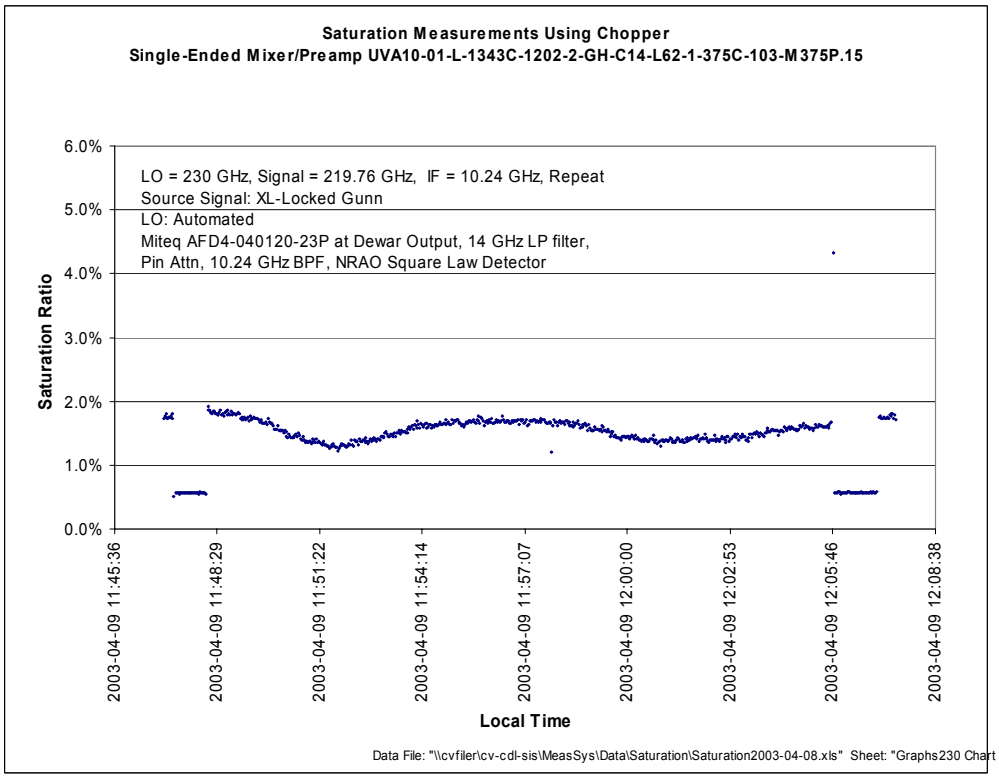

Figure 13: Saturation with LO = 230 GHz, LSB, repeat of Figure 12

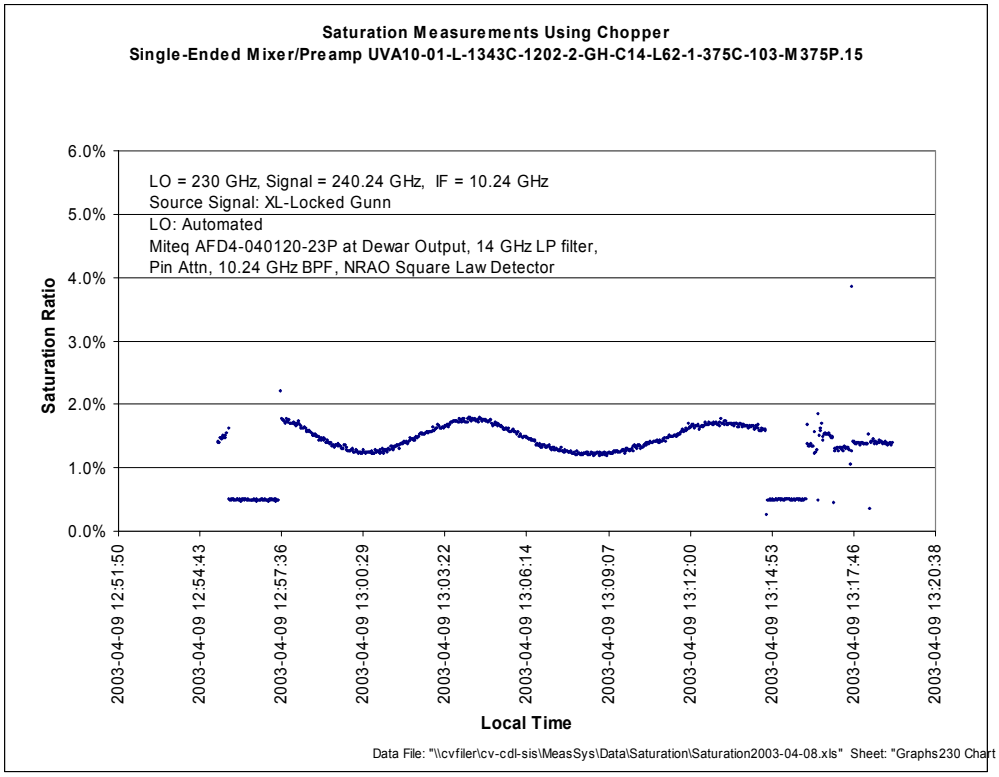

Figure 14: Saturation with LO = 230 GHz, USB.

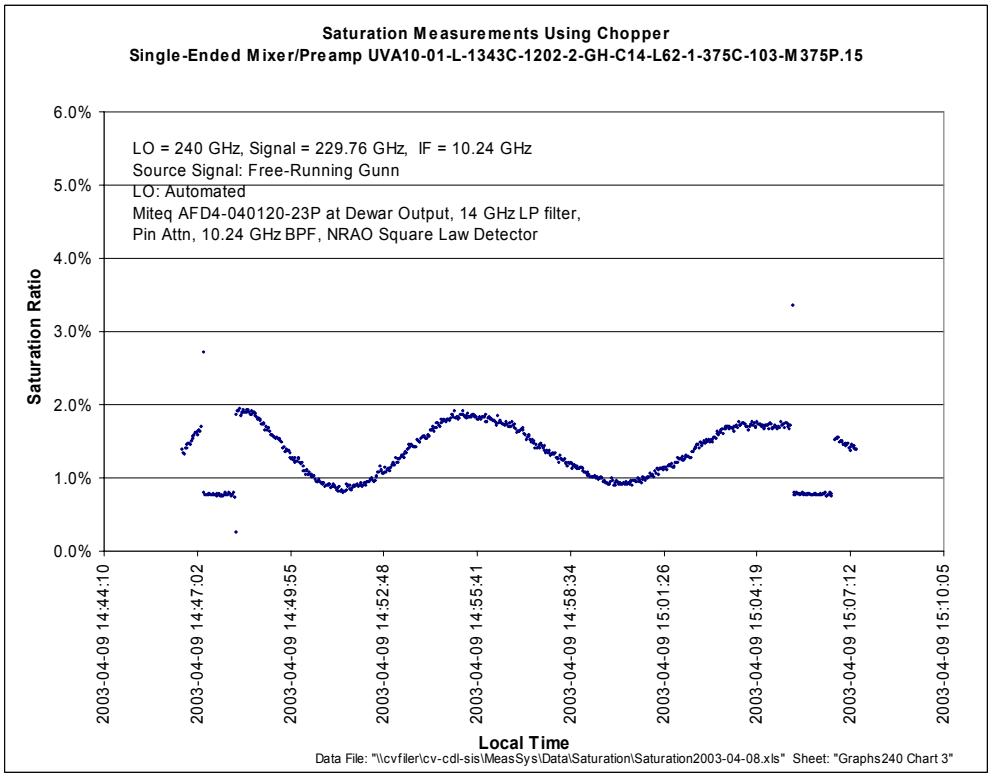

Figure 15: Saturation with LO = 240 GHz, LSB

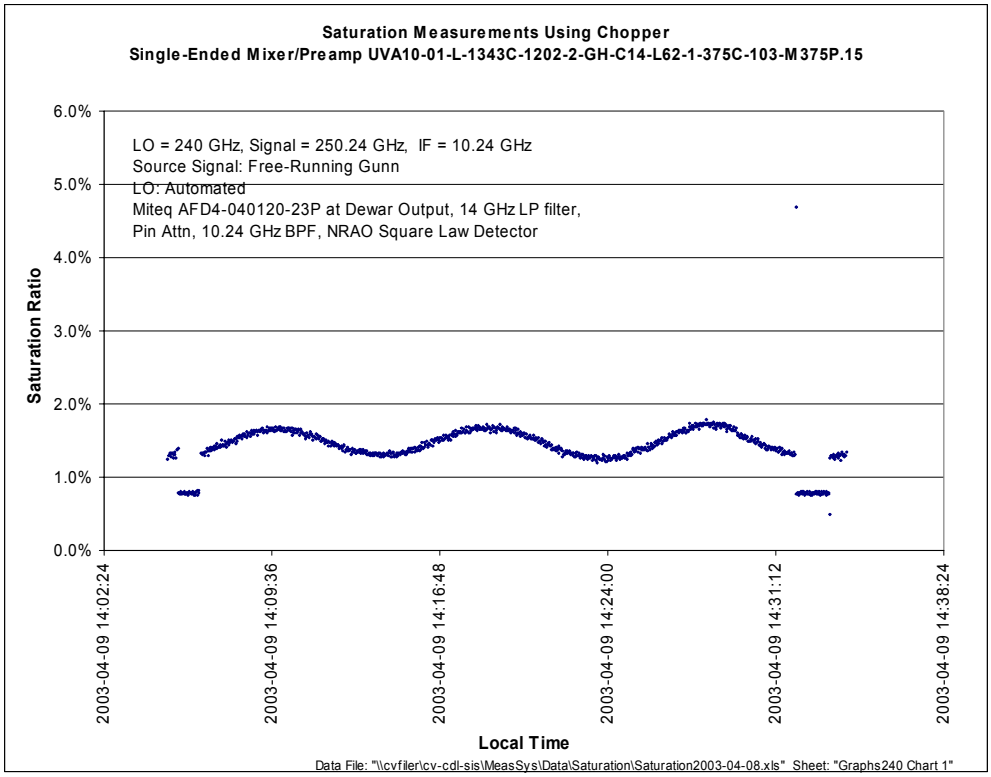

Figure 16: Saturation with LO = 240 GHz, USB

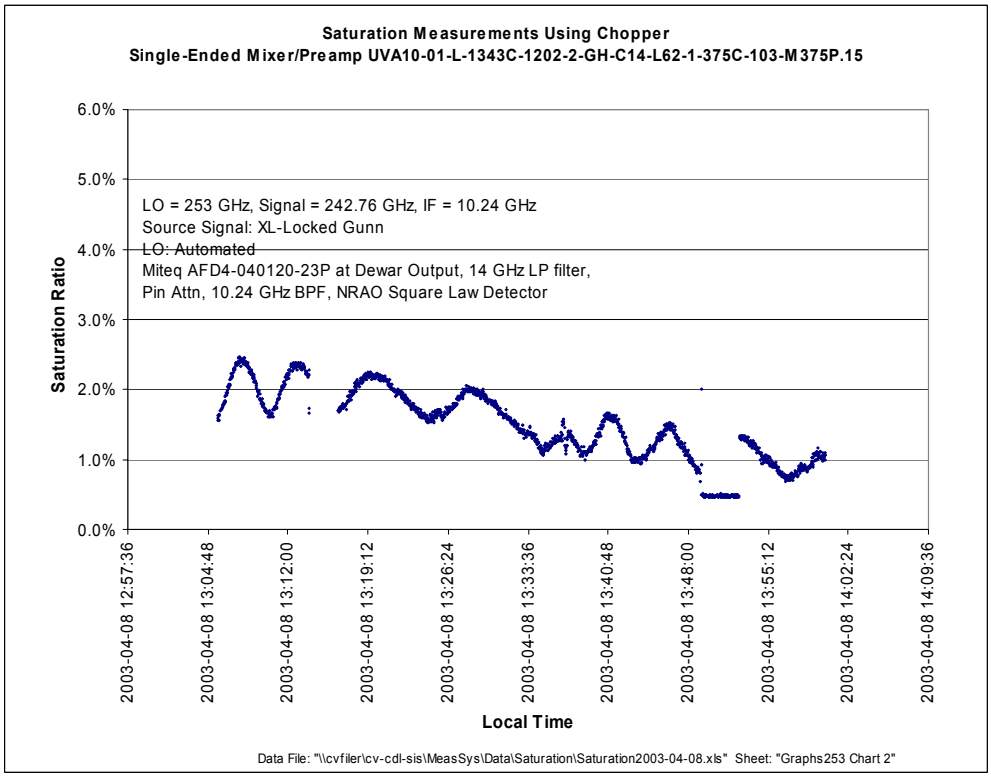

Figure 17: Saturation with LO = 253 GHz, LSB

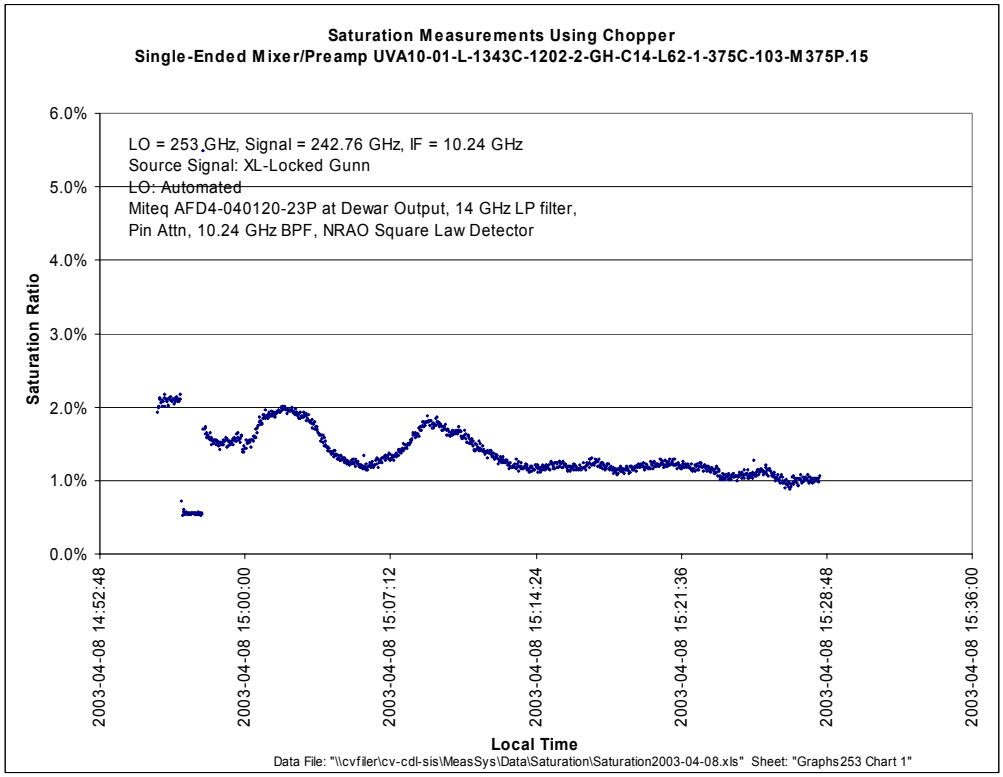

Figure 18: Saturation with LO = 253 GHz, LSB, Repeat of data in Figure 17.

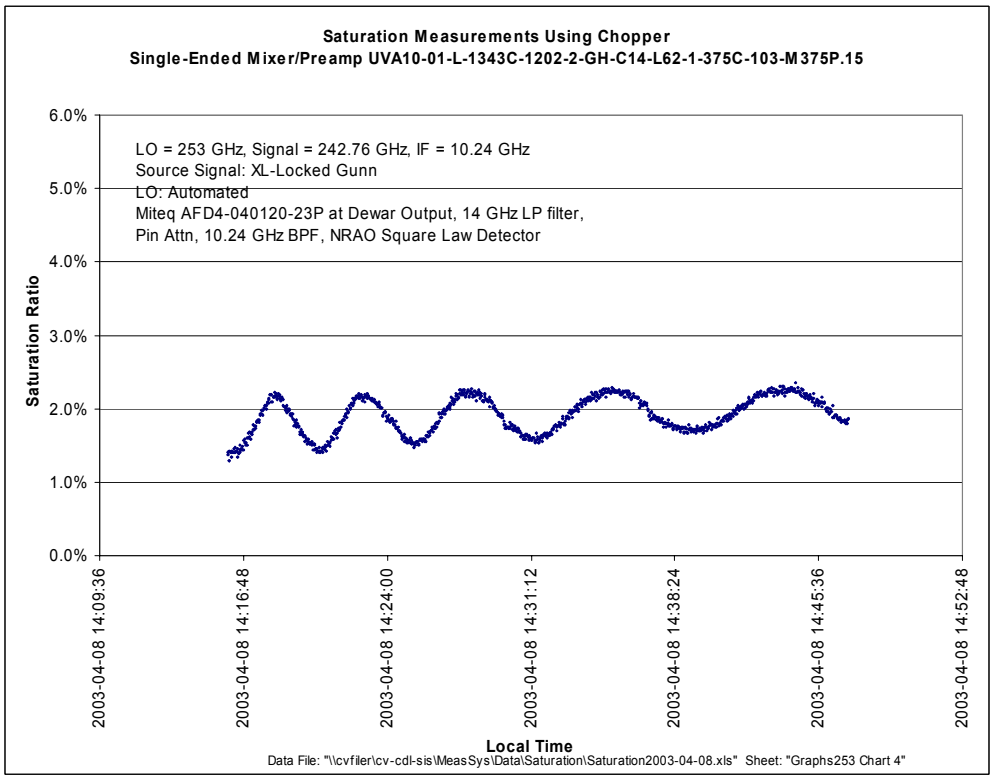

Figure 19: Saturation with LO = 253 GHz, LSB, Repeat of data in Figure 17.

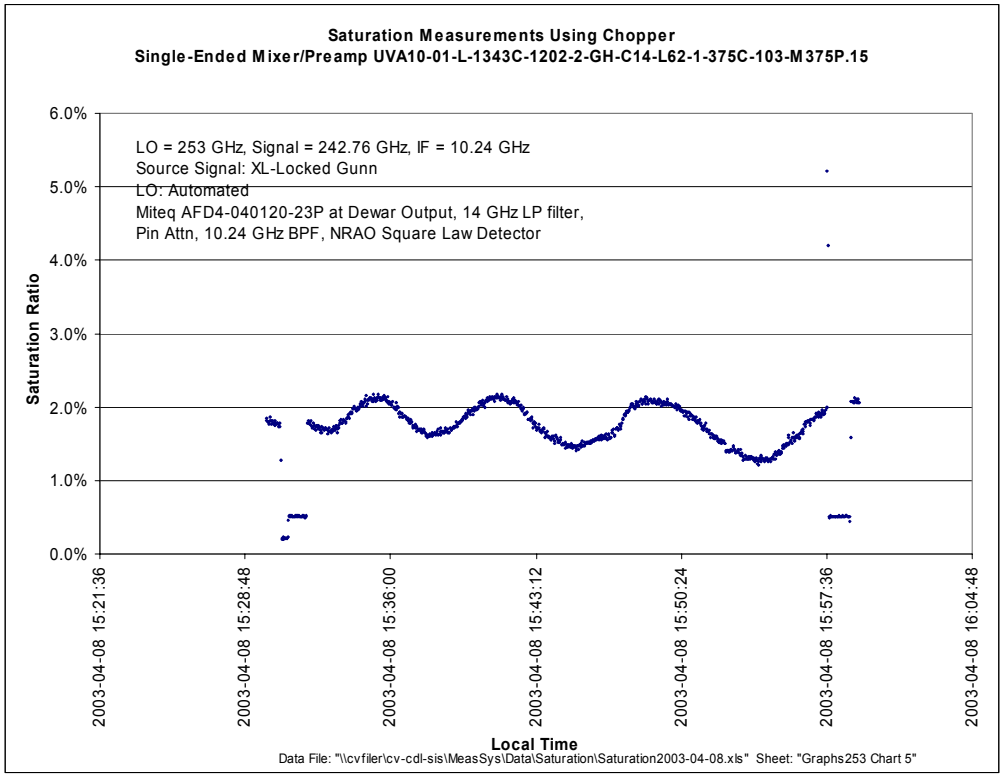

Figure 20: Saturation with LO = 253 GHz, LSB, Repeat of data in Figure 17

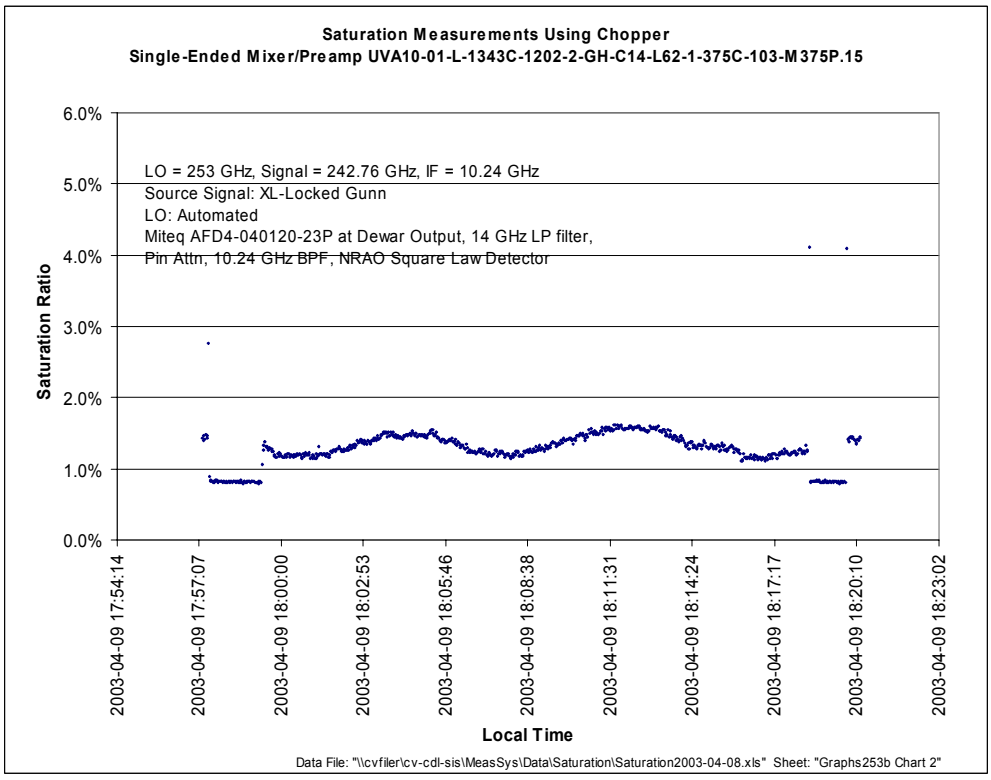

Figure 21: Saturation with LO = 253 GHz, LSB, Repeat of data in Figure 17

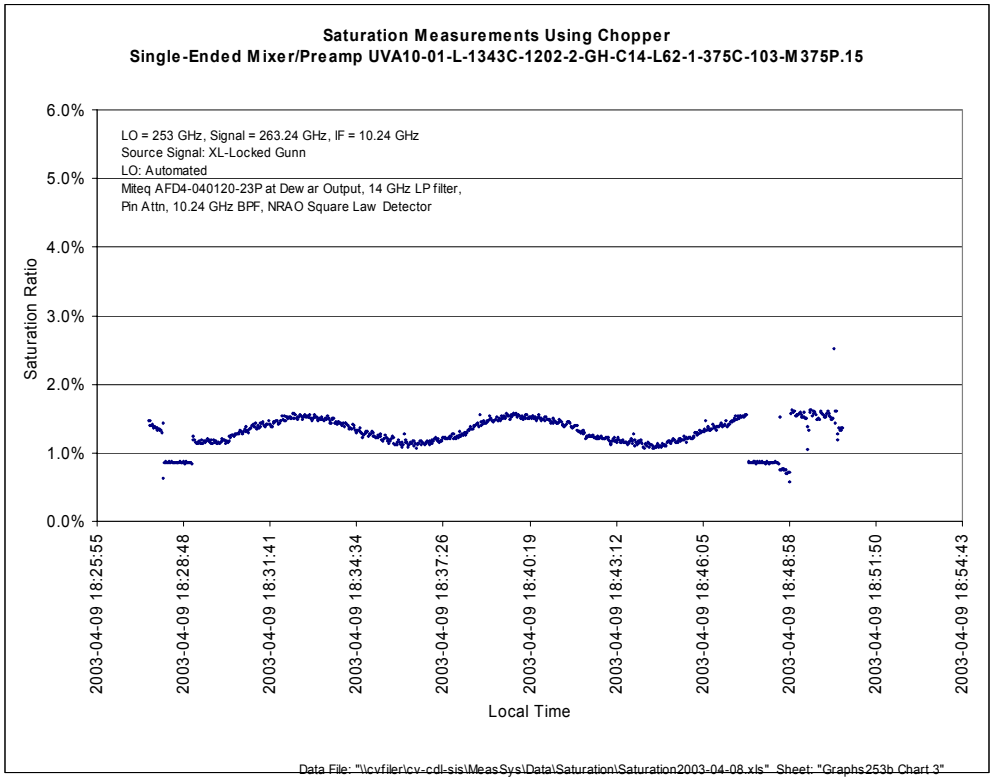

Figure 22: Saturation with LO = 253 GHz, USB. Signal reduced approximately 4 dB at end of sweep.

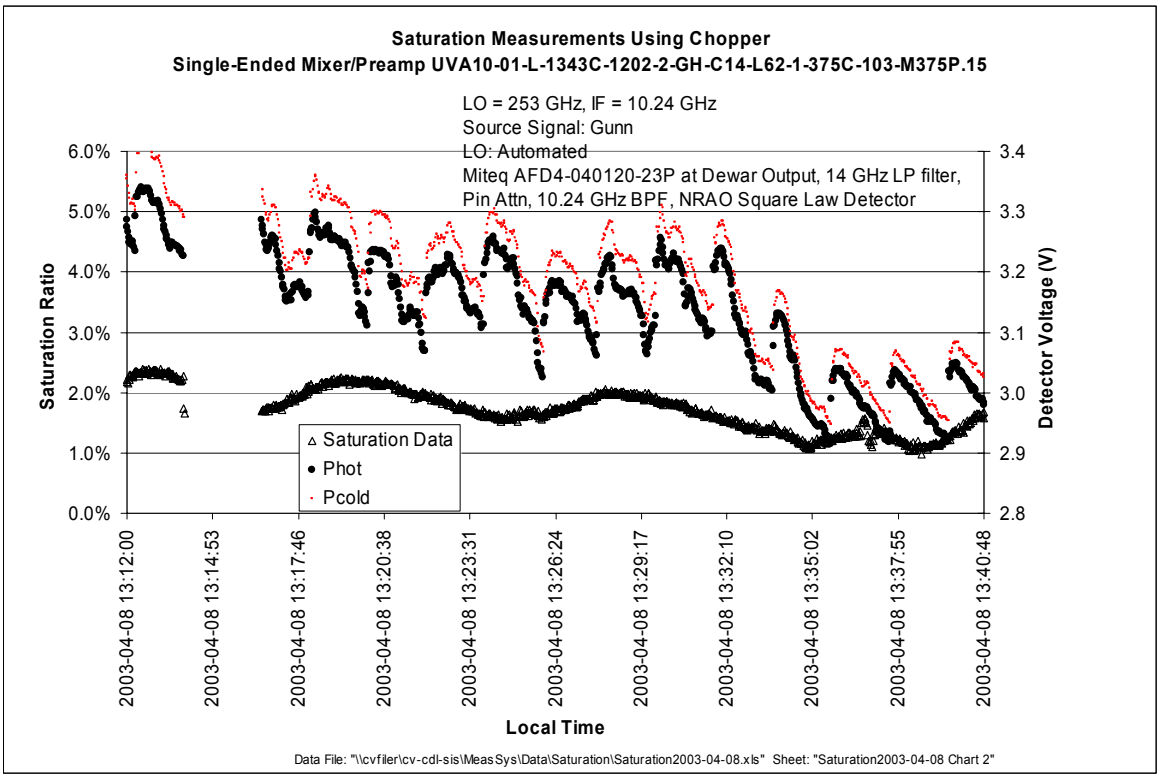

Figure 23: Investigation of saturation drift for a LO=253 GHz. Repeat of Figure 17 with superimposed square law detector voltages. The curves labeled "P_{hot}" and "P_{cold}" are voltage outputs from the square law detector. The period of the ripple is approximately two minutes.

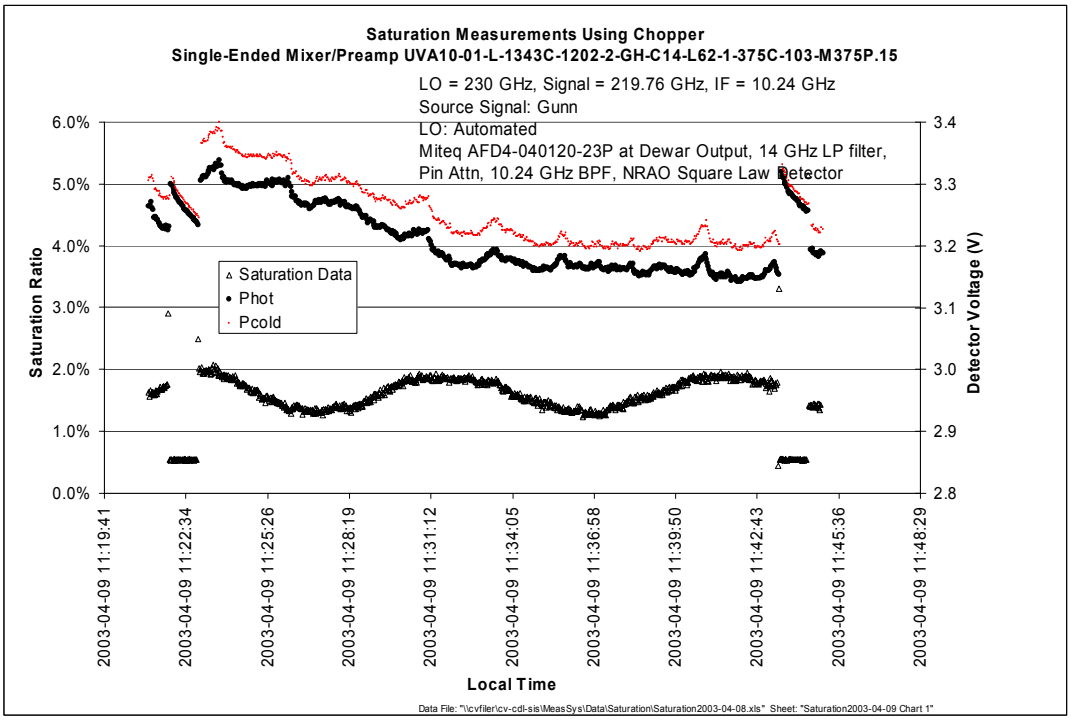

Figure 24: Investigation of saturation drift for a LO=230 GHz. Repeat of Figure 13 with square law detector voltage superimposed on data.

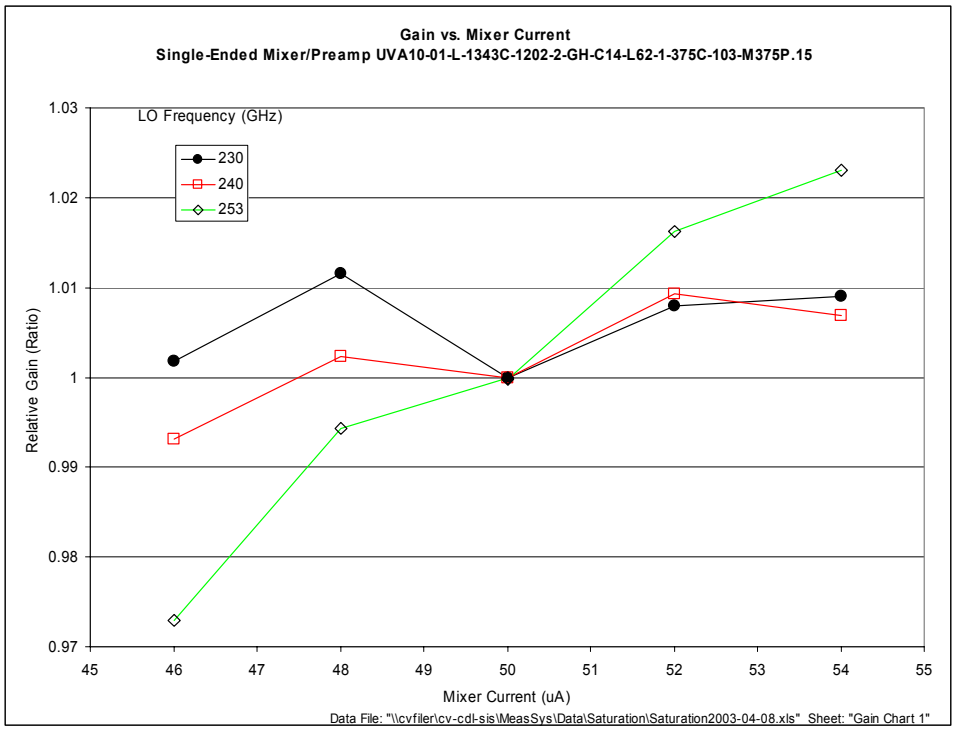

Figure 25: Gain of Mixer-Preamp *vs.* Mixer Current